PNAS
www.pnas.org

Supplementary Information for

Light-induced *psbA* translation in plants is triggered by photosystem II damage via an assembly-linked autoregulatory circuit

Prakitchai Chotewutmontri and Alice Barkan

Alice Barkan
Email: abarkan@uoregon.edu

This PDF file includes:

SI Materials and Methods
Figures S1 to S4
Legend for Dataset S1
SI References

Other supplementary materials for this manuscript include the following:

Dataset S1

www.pnas.org/cgi/doi/10.1073/pnas.2007833117

SI Materials and Methods

Plant Material. Maize seedlings were grown under cycles of 16-h light at 28°C and 8-h dark at 26°C with light intensity of 250-350 μmol m^{-2} s^{-1} (mixture of fluorescent Sylvania F72T12/CW/VHO or F48T12/CW/HO with incandescent Sylvania 100A/DLSW/VERT/RP) for ~8 days, when the third leaf was emerging from the leaf whorl. Phenotypically normal siblings were used as the wild-type controls. Arabidopsis seeds were grown on 1x MS medium supplemented with 2 or 3% (w/v) sucrose and 0.3% (w/v) Phytagel, pH 5.7. Plants used for the *hcf107, hcf136,* action spectrum, nigericin, and CCCP treatments were grown in short days (10-h light/14-h dark) at 22˚C and were harvested after 14 days (*hcf107* and *hcf136*), 18 to 21 days (action spectrum, varied among replicates), or 23 days (nigericin and CCCP). Plants used for the At-*psa3, hcf208,* and DCMU experiments were grown in long days (16-h light/8-h dark) at 22 ˚C for 16, 16, and 14 days, respectively. Plants used for the analysis of the *stn7-stn8* double mutant were grown in 12 h light/12 h dark for 15 days. A light intensity of 80-100 μmol m^{-2} s^{-1} (fluorescent Sylvania F72T12/CW/VHO or F48T12/CW/HO) was used for Arabidopsis growth, except in the case of the *hcf208* line, which was grown under lower light intensity (30-50 μmol m^{-2} s^{-1}) to increase PSII abundance. Phenotypically normal siblings were used as wild-type controls except in the *stn7-stn8* experiment, which used the Col-0 progenitor as the wild-type.

Effects of monochromatic light sources on translation. Leaves from four seedlings were pooled for each ribo-seq sample and leaves from two or three seedlings were pooled for pulse labeling. The following sources were used for supplemental lighting: 25 μmol m^{-2} s^{-1} white light (incandescent bulb Sylvania 100A/DLSW/VERT/RP), 5 μmol m^{-2} s^{-1} UV-B (M-26XV Benchtop Variable Transilluminator, UVP), 5 μmol m^{-2} s^{-1} UV-A (UVL-56 Handheld UV Lamp, UVP), 5 μmol m^{-2} s^{-1} blue, green or red light emitting diodes (LEDs) (Remix Headlamps, Princeton Tec) with maximum emission wavelengths (λ) of 314, 370, 469, 522 and 635 nm, respectively. The spectra of UV-A and UV-B lights were determined using a CCS200 Compact Spectrometer (Thorlabs) from 195 to 1020 nm and FLAME-S-UV-VIS-ES Spectrometer (Ocean Optics) from 180 to 880 nm, respectively. The spectra of LEDs were determined with a CCS200 Compact Spectrometer (Thorlabs) from 195 to 1020 nm and an ILT350 Illuminance Spectrometer (International Light Technology) from 380 to 780 nm; the ILT350 spectra are shown in Figure 1*A*. The spectra of basal and supplemental white lights were determined with an ILT350 Illuminance Spectrometer (International Light Technology) from 380 to 780 nm. Average spectra from at least three measurements are shown in Figure 1*A*. The intensities of white lights and LEDs with wavelengths within the photosynthetically active radiation (PAR) range were determined using a MQ-200 quantum meter (Apogee Instruments). To determine the intensities of UV-A and UV-B, the light energy flux (irradiance in W cm^{-2}) was measured using an ILT1700 Research Radiometer (International Light Technology). The light photon energy (E_p) was calculated using the maximum emission wavelength from $E_p = hc / \lambda$ where *h* is Planck's constant and *c* is speed of light. The light intensity (μmol photon m^{-2} s^{-1}) is the irradiance I / (E_p x Avogadro constant).

***In Vivo* Pulse Labeling.** Details for specific experiments were as follows. A light intensity of 8 μmol m^{-2} s^{-1} (Sylvania F40/D41/SS) was used for the drug treatments. A light intensity of 100 μmol m^{-2} s^{-1} (AgroMax F24/T5/HO) was used for mutant assays. Light conditions for the action spectrum analyses are indicated in figures. Unless otherwise indicated, rosette leaves from two to three seedlings (approximately two weeks post germination, 6-8 leaves per labeling) were excised and placed in a clear 24-well plastic plate containing 135 μl of labeling buffer (100 μg/mL cycloheximide, 1x MS medium, 2% (w/v) sucrose, pH 5.7). 15 μl of EasyTag Express ^{35}S Protein Labeling Mix (Perkin Elmer) was added immediately to initiate labeling. For *uvr8*, the young leaves from 55-day-old plants were used for labeling (total of 6-8 leaves pooled from 2 plants per labeling). For the *stn7-stn8* mutant, leaves were pre-incubated for 30 min in labeling buffer containing 25 μg/mL cycloheximide prior to addition of the radiolabeled amino acids. After the 20 min labeling period, leaves were washed twice in labeling buffer lacking radiolabeled amino acids and frozen in liquid nitrogen. The homogenization buffer was as described previously (1), with 5 mM $MgCl_2$ added for the At-*psa3* and At-*hcf208* experiments to improve recovery of thylakoid membranes in the pellet. The membrane fraction was collected by centrifugation at 10,000 x g for

5 min at 4°C. The supernatant, which includes some membrane contamination, was designated in Figure 3*C* as the Soluble plus Low Density Membrane fraction. We suspect that the membrane component comes primarily from stromal lamellae. Membrane fractions were washed twice and then resolved on 11% polyacrylamide SDS-PAGE gels containing 6 M urea, whereas total leaf extracts were resolved on 4-20% polyacrylamide SDS-PAGE gels.

Ribo-seq and RNA-seq. Ribosome footprints were prepared as described previously (1). In brief, RNase I was used to generate monosomes, monosomes were pelleted through a sucrose cushion, RNA was extracted from the pelleted material, RNA between 20 and 40 nucleotides was gel purified, and the gel-purified RNA was used as input for the NEXTflex Small RNA Sequencing Kit v3 (Perkin Elmer). rDNA depletion was performed using species-specific sets of biotinylated DNA oligonucleotides (1). Aliquots of the same tissue homogenates were used for RNA-seq. For RNA-seq, rRNA was depleted with the Ribo-Zero rRNA Removal Kit (Plant Leaf) (Illumina), and libraries were prepared with the NEXTflex qRNA-Seq Kit v2 (Perkin Elmer) (DCMU, Zm-*hcf136* and At-*hcf136* samples) or the NEXTflex Rapid Directional qRNA-Seq Kit (Perkin Elmer) (At-*hcf107* samples). Libraries were sequenced on a HiSeq 4000 instrument (Illumina), with read lengths of 75 or 100 nucleotides.

Sequencing data were processed as described in (2) with the following modifications. Trimmed reads were sequentially aligned to the chloroplast, mitochondrial and nuclear genomes using STAR (3) instead of Bowtie 2. Maize reads were aligned to GenBank accession X86563 (chloroplast genome) and B73 RefGen_v4 assembly version 38 (maizegdb.org) (nucleus and mitochondria). Arabidopsis reads were aligned to the TAIR10 genome and annotation (arabidopsis.org). Read counting was performed using featureCounts (4) instead of the in-house scripts used previously. Read counts for chloroplast genes excluded the first 10 nucleotides of each ORF to avoid counting the ribosome pileup at the start codon. Chloroplast read counts were normalized by using reads per kilobase of coding sequence (CDS) per million reads mapped to all chloroplast CDSs (cpRPKM). Read mapping statistics and cpRPKM values from all the experiments are provided in *SI Appendix,* Dataset S1.

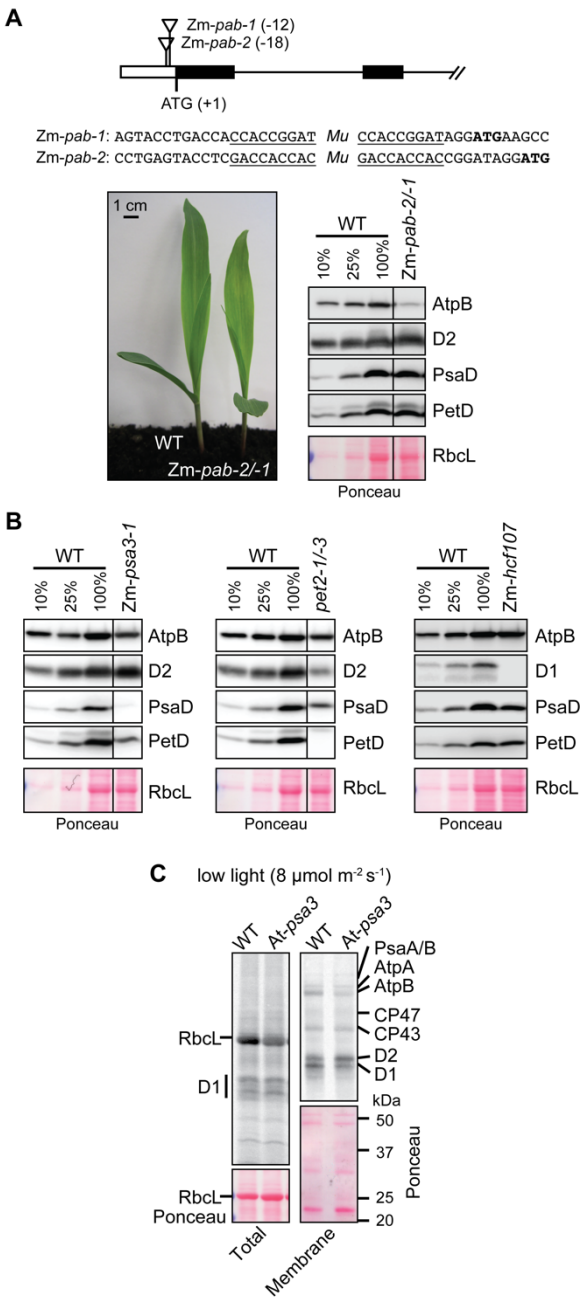

Fig. S1. Additional information about mutants analyzed in Figures 3, 4, and 5. (*A*) Maize *pab* mutants. Two transposon insertion alleles were recovered from the Photosynthetic Mutant Library (5). The position of the insertions with respect to the start codon is diagrammed, and the sequences of the insertion sites are shown with the target site duplications underlined. The heteroallelic progeny of a complementation test cross (Zm-*pab-2/-1*) were used for the experiments here. The phenotype of seedlings at the stage used here (grown for 8 days in soil) is shown. The immunoblots to the right show the abundance of representative core subunits of photosynthetic complexes. Replicate blots were probed to detect AtpB (subunit of the chloroplast ATP synthase), D2 (subunit of PSII), PsaD (subunit of PSI), and PetD (subunit of the cytochrome b_6f complex). An excerpt of one of the Ponceau S-stained blots illustrates relative sample loading and the abundance of the large subunit of Rubisco (RbcL). The specific loss of AtpB is as expected based on analysis of the orthologous mutant in Arabidopsis (6). Lines separate non-contiguous lanes from the same exposure of the same blot. (*B*) Immunoblot validation of maize

mutants used here that were reported previously (7-9). Lines separates non-contiguous lanes from the same exposure of the same blot. (*C*) Pulse labeling of At-*psa3* in low intensity light (8 μmol m^{-2} s^{-1}). Labeling was performed in the presence of cycloheximide for 20 min. Total leaf lysates (left) and membrane fractions (right) were resolved by SDS-PAGE and transferred to nitrocellulose, and radiolabeled proteins were detected by phosphorimaging. The imaged blots were also stained with Ponceau S to illustrate relative sample loading.

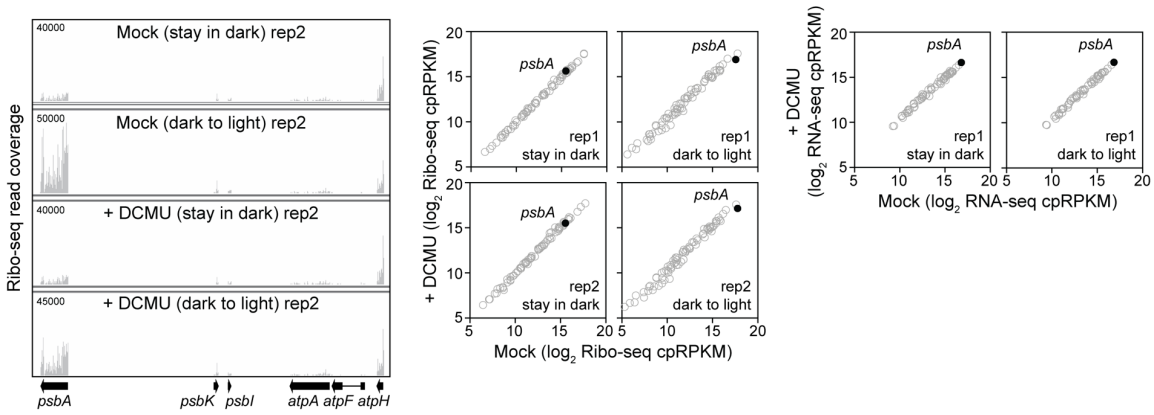

Fig. S2. Additional data to support the DCMU experiment shown in Figure 5*A*. Arabidopsis (Col-0) was treated with DCMU as shown in Fig. 4*C*. The left panel shows Integrated Genome Viewer (IGV) screen captures from a replicate of the ribo-seq experiment shown in Fig. 5*A*. Middle panels show scatter plot comparisons of ribosome footprint abundance for all chloroplast genes in the DCMU-treated and untreated (mock) samples. Right panels show scatter plots comparing mRNA abundance (RNA-seq) for all chloroplast genes in the DCMU-treated and untreated (mock) samples. RNA was prepared from the same lysates used for ribo-seq. Each symbol represents one gene. Values are expressed as reads per kilobase in the ORF per million reads mapped to chloroplast ORFs (cpRPKM).

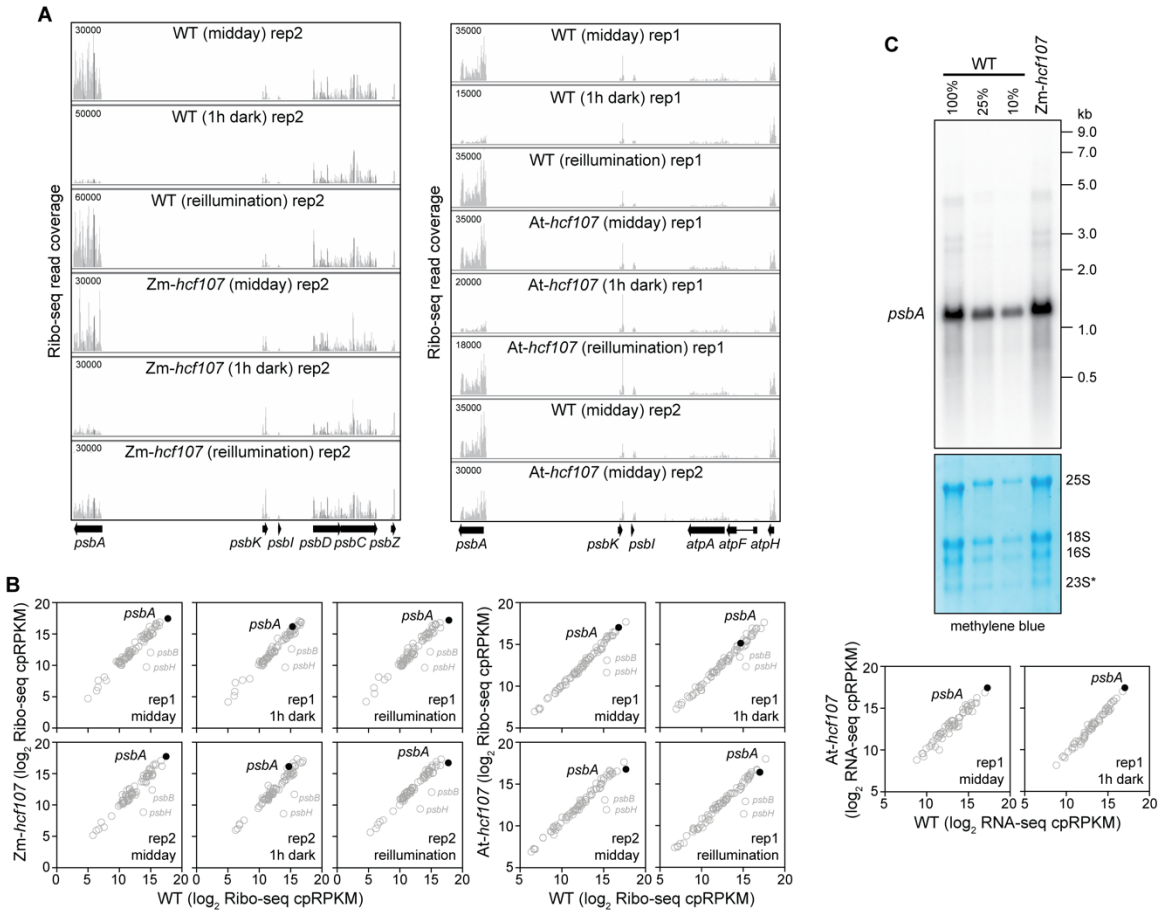

Fig. S3. Additional data to support the ribo-seq analysis of At-*hcf107* and Zm-*hcf107* mutants shown in Figure 5*B.* The experiments were performed as described in Fig. 5*B*. *(A)* Screen captures from the Integrated Genome Viewer (IGV) showing the distribution of ribosome footprints along *psbA* and adjacent ORFs. The maximum Y-axis values are shown in the upper left, and were chosen such that coverage of adjacent ORFs were similar. *(B)* Scatter plots comparing ribosome footprint abundance for all chloroplast genes in the mutant and its phenotypically normal siblings (WT). Each symbol represents one gene. Values are expressed as reads per kilobase in the ORF per million reads mapped to chloroplast ORFs (cpRPKM). The second replicate of the Arabidopsis midday analysis was published previously (8). *(C)* Abundance of *psbA* mRNA in *hcf107* mutants. The top panel shows RNA gel blot hybridization analysis of Zm-*hcf107* and phenotypically normal siblings (WT) from tissue harvested at midday. The blot was stained with methylene blue to image rRNA abundance and then hybridized with a probe specific for maize *psbA* (GenBank Accession X86563 nucleotide positions 295-1074). Bottom panels show scatter plots comparing mRNA abundance (RNA-seq) for all chloroplast genes in At-*hcf107* and phenotypically normal siblings (WT). RNA was prepared from the same lysates used for ribo-seq. Each symbol represents one gene. Values are expressed as reads per kilobase in the ORF per million reads mapped to chloroplast ORFs (cpRPKM).

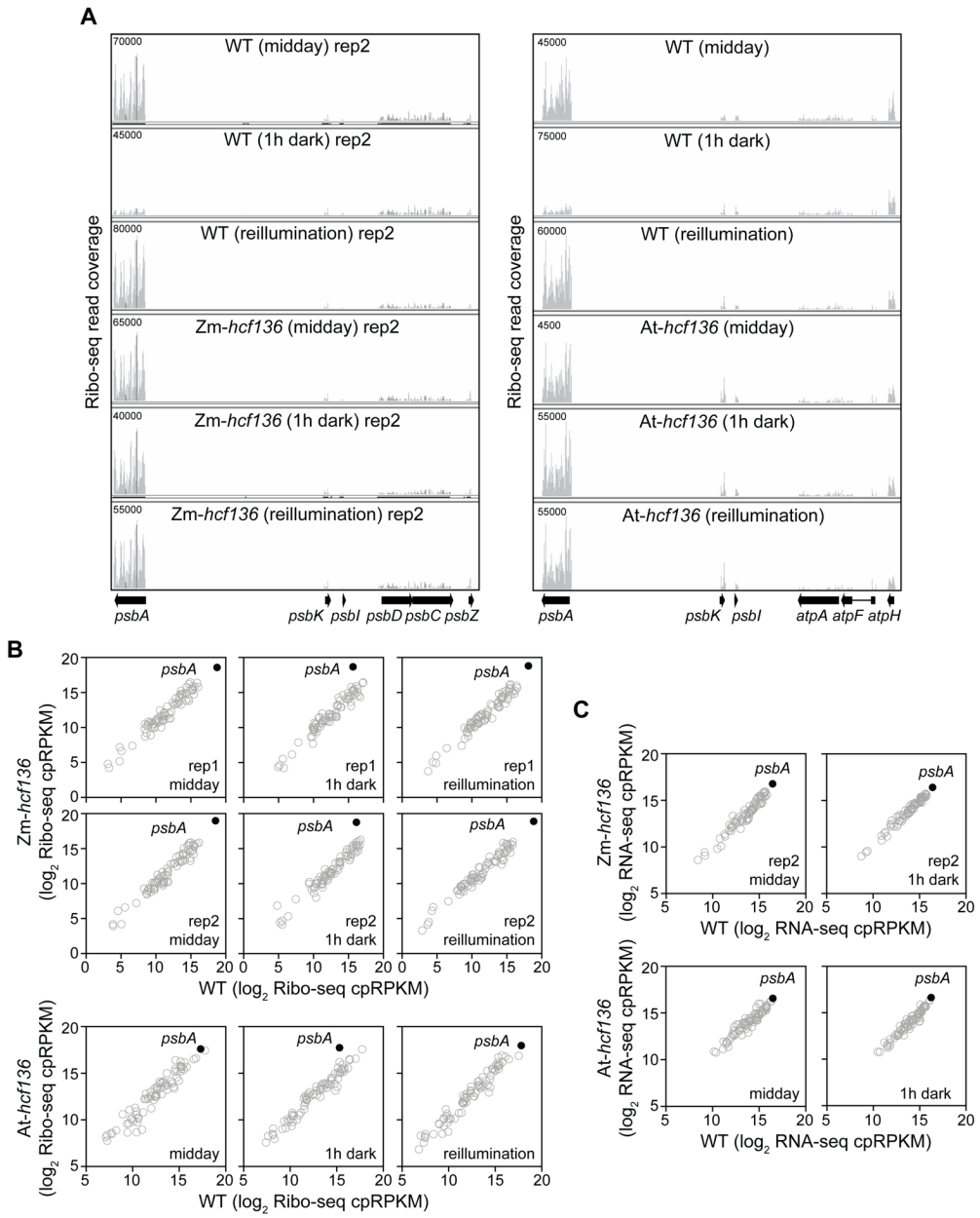

Fig. S4. Additional data to support the ribo-seq analysis of At-*hcf136* and Zm-*hcf136* mutants shown in Figure 5*C*. The results from the midday samples were published previously (10), but these were analyzed in parallel with the corresponding 1-h dark and 15-min reillumination samples. (*A*) Screen captures from the Integrated Genome Viewer (IGV) showing the distribution of ribosome footprints along *psbA* and adjacent ORFs. The maximum Y-axis values are shown in the upper left, and were chosen such that coverage of adjacent ORFs were similar. *(B)* Scatter plots comparing ribosome footprint abundance for all chloroplast genes in the mutant and its phenotypically normal siblings (WT). Each symbol represents one gene. Values are expressed as reads per kilobase in the ORF per million reads mapped to chloroplast ORFs (cpRPKM). *(C)* Scatter plots comparing mRNA abundance (RNA-seq) for all chloroplast genes in the mutant and its phenotypically normal siblings (WT). RNA was prepared from the same lysates used for ribo-seq. Each symbol represents one gene. Values are expressed as reads per kilobase in the ORF per million reads mapped to chloroplast ORFs (cpRPKM).

Dataset S1 (separate file). Summary of Ribo-seq and RNA-seq data**.**

SI References

1. P. Chotewutmontri, A. Barkan, Multilevel effects of light on ribosome dynamics in chloroplasts program genome-wide and *psbA*-specific changes in translation. *PLoS Genet* **14**, e1007555 (2018).
2. P. Chotewutmontri, A. Barkan, Dynamics of chloroplast translation during chloroplast differentiation in maize. *PLoS Genet* **12**, e1006106 (2016).
3. A. Dobin, C. A. Davis, F. Schlesinger, J. Drenkow, C. Zaleski, S. Jha, P. Batut, M. Chaisson, T. R. Gingeras, STAR: ultrafast universal RNA-seq aligner. *Bioinformatics* **29**, 15-21 (2013).
4. Y. Liao, G. K. Smyth, W. Shi, featureCounts: an efficient general purpose program for assigning sequence reads to genomic features. *Bioinformatics* **30**, 923-930 (2014).
5. S. Belcher, R. Williams-Carrier, N. Stiffler, A. Barkan, Large-scale genetic analysis of chloroplast biogenesis in maize. *Biochim Biophys Acta* **1847**, 1004-1016 (2015).
6. J. Mao, W. Chi, M. Ouyang, B. He, F. Chen, L. Zhang, PAB is an assembly chaperone that functions downstream of chaperonin 60 in the assembly of chloroplast ATP synthase coupling factor 1. *Proc Natl Acad Sci U S A* **112**, 4152-4157 (2015).
7. J. Shen, R. Williams-Carrier, A. Barkan, PSA3, a protein on the stromal face of the thylakoid membrane, promotes Photosystem I accumulation in cooperation with the assembly factor PYG7. *Plant Physiol* **174**, 1850-1862 (2017).
8. R. Williams-Carrier, C. Brewster, S. Belcher, M. Rojas, P. Chotewutmontri, S. Ljungdahl, A. Barkan, The Arabidopsis pentatricopeptide repeat protein LPE1 and its maize ortholog are required for translation of the chloroplast *psbJ* RNA. *Plant J* **99**, 56-66 (2019).
9. R. Williams-Carrier, N. Stiffler, S. Belcher, T. Kroeger, D. B. Stern, R. A. Monde, R. Coalter, A. Barkan, Use of Illumina sequencing to identify transposon insertions underlying mutant phenotypes in high-copy Mutator lines of maize. *Plant J* **63**, 167-177 (2010).
10. P. Chotewutmontri, R. Williams-Carrier, A. Barkan, Exploring the link between photosystem II assembly and translation of the chloroplast *psbA* mRNA. *Plants* **9**, pii: E152 (2020).